Renewable and Sustainable Energy Reviews 16 (2012) 1636–1656

Contents lists available at SciVerse ScienceDirect

Renewable and Sustainable Energy Reviews

journal homepage: www.elsevier.com/locate/rser

Computing global and diffuse solar hourly irradiation on clear sky. Review and testing of 54 models

Viorel Badescu[a,*], Christian A. Gueymard[b], Sorin Cheval[c], Cristian Oprea[d], Madalina Baciu[d], Alexandru Dumitrescu[d,e], Flavius Iacobescu[a], Ioan Milos[d], Costel Rada[d]

[a] Candida Oancea Institute, Polytechnic University of Bucharest, Spl. Independentei 313, Bucharest 060042, Romania
[b] Solar Consulting Services, P.O. Box 392, Colebrook, NH 03576, USA
[c] National Research and Development Institute for Environmental Protection, Splaiul Independentei nr. 294, Sect. 6, Bucuresti 060031, Romania
[d] National Meteorological Administration, 97 Sos. Bucuresti-Ploiesti, Bucharest 013686, Romania
[e] University of Bucharest, Faculty of Geography, Bucharest, Romania

A R T I C L E I N F O

Article history:
Received 14 December 2011
Accepted 18 December 2011
Available online 18 January 2012

Keywords:
Clear sky models
Global solar radiation
Diffuse solar radiation
Hourly irradiation
Romania

A B S T R A C T

Fifty-four broad band models for computation of global and diffuse irradiance on horizontal surface are shortly presented and tested. The input data for these models consist of surface meteorological data, atmospheric column integrated data and data derived from satellite measurements. The testing procedure is performed for two meteorological stations in Romania (South-Eastern Europe). The testing procedure consists of forty-two stages intended to provide information about the sensitivity of the models to various sets of input data. There is no model to be ranked "the best" for all sets of input data. Very simple models as well as more complex models may belong to the category of "good models". The best models for solar global radiation computation are, on equal-footing, ESRA3, Ineichen, METSTAT and REST2 (version 81). The second best models are, on equal-footing, Bird, CEM and Paulescu & Schlett. The best models for solar diffuse radiation computation are, on equal-footing, ASHRAE2005 and King. The second best model is MAC model. The best models for computation of both global and diffuse radiation are, on equal-footing, ASHRAE 1972, Biga, Ineichen and REST2 (version 81). The second best is Paulescu & Schlett model.

Contents

* Corresponding author. Tel.: +40 21 402 9339; fax: +40 21 318 1019.
E-mail addresses: badescu@theta.termo.pub.ro (V. Badescu), Chris@SolarConsultingServices.com (C.A. Gueymard), sorincheval@yahoo.com (S. Cheval).

1364-0321/$ – see front matter
doi:10.1016/j.rser.2011.12.010

1. Introduction

The appropriate design of many solar energy devices requires a detailed knowledge of solar global and diffuse radiation availability. Although there are several world maps of solar radiation, they are not detailed enough to be used for the determination of available solar energy on small areas. These circumstances have prompted the development of calculation procedures to provide radiation estimates for areas where measurements are not carried out and for situations when gaps in the measurement records occurred. Only a minority of these procedures has been validated by their authors, and usually under specific geographical or climatic circumstances only. To increase the confidence in modeled data accuracy there is a need for validation by independent groups and at a variety of test sites in many different climatic areas. Existing validation reports of the literature refer usually to a small number of models being inter-compared under specific climatic environments [1–10]. The correct validation and comparison of radiative models raise specific issues. For instance, different statistics may be used to evaluate the bias and random differences between the computed and measured data. Moreover, various ranking procedures can be used to compare the performance of models, yielding different results (for more detailed discussions, see [9]).

One problem occurring during models utilization is the large variety of input data that various users has at their disposal. It is quite usual that the user has access to databases which do not cover all the necessary input parameters of a specific model known to have good performance. In this case the user has to choose another model which fits the available input databases or, alternately, to prepare ad hoc input parameters for that specific model. This last solution sometimes involves data interpolation (or even extrapolation) and lower overall performance is then expected due to unavoidable propagation of errors.

The present investigation considers 54 clear-sky global and diffuse solar radiation models, i.e. a much larger sample of what the literature offers than in any previous study. Most of these models have been previously tested, under a few geographical conditions, during different time intervals and by using various testing procedures. How they compare in practice under specific and identical conditions is still not known.

Reference radiometric measurements (used as “ground truth”) are provided here by two meteorological and radiometric stations in South-Eastern Europe (Romania). These stations have provided good-quality routine data over many years. These are not high-end research-class stations, however, which means that the present study can be considered representative of what can be obtained at hundreds of similar stations over the world, rather than at a few specialized sites, like in some previous studies (e.g. [9,10]). These studies considered the ideal case when all the investigated models' inputs were measured locally at high frequency with high-quality instruments, so as to obtain the intrinsic performance of these models by avoiding propagation of errors. In contrast, the present investigation is much more pragmatic, since it uses “normal” radiation measurements and interpolated/extrapolated input data in both space and time to evaluate the “real world” performance of models under non-ideal conditions. Results have been presented for computation of global radiation [11] and diffuse radiation [12].

The objectives of this investigation are twofold. First, a review of models performance is made, by comparing their predictions under identical climate conditions and using a unique testing procedure for computation of global and diffuse radiation. Second, the sensitivity of each model's performance on the accuracy in the atmospheric databases used as inputs is reported for both types of solar radiation.

2. Models

All the 54 models for computation of global and diffuse irradiance on horizontal surface are briefly described in what follows, using a call number (G001 to G054) for further reference. Some of these models were already tested in [9,10,13]. Fortran routines for all models may be found in [11,12]. The only input variable that is common to all models is the zenith angle, *Z*, which characterizes the sun position. For those models that refer to the solar constant, a common value of 1366.1 W/m^2 is used [14].

G001. ASHRAE 1972

This is a historical model still widely used by engineers to calculate solar heat gains and cooling loads in buildings, or insolation of simple solar systems. It is based on original empirical work conducted in the 1950s and 1960s [15]. For more details, see [3,10].

G002. ASHRAE 2005

ASHRAE 2005 is similar to ASHRAE model of 1972, but with some revised coefficients that appeared in [16].

G003. Badescu

This model is based on MAC (entry G029 in this list), and was proposed by Badescu [17].

G004. Bashahu

The composite model of Bashahu and Laplaze [18] is based on the direct irradiance model of King and Buckius [19]; see entry G027 below.

G005. BCLSM

This is the model originally proposed by Barbaro et al. [20] and later modified in [1,4,21]. The original Barbaro equations are used here, with three modifications: (1) The units in Barbaro's Eq. (10) are converted from cal/(cm^2 min) to W/m^2, using 1 cal = 4.184 J; (2) a multiplier of 0.1 that was apparently missing in the second part

of Eq. (10) has been added; and (3) Barbaro's Eq. (11) has been corrected for the missing $\cos Z$ term involving the zenith angle Z.

G006. Biga

This is the model proposed by Biga and Rosa [22].

G007. Bird model

This is the broadband transmittances and turbidity model according to Bird and Hulstrom [23,24]. For more details, see [10,25].

G008. CEM

This is the broadband model proposed in Atwater and Ball [26,27]. See details in [25].

G009. Chandra

In this model proposed by Chandra [28], the Linke turbidity coefficient, T_L, was originally a necessary input. This coefficient is obtained here from an average of four linear relationships between Angstrom's β coefficient and T_L, as proposed in [29–32]:

$$T_L = 2.1331 + 19.0204\beta. \tag{1}$$

T_L must be constrained to the range 2–5 to avoid divergence in Chandra's model. Chandra reported his results as absolute irradiances in cal/(cm^2 min), and used a solar constant of 1.94 cal/(cm^2 min) or 1353 W/m^2. His results are therefore divided here by 1.94 to obtain transmittances. This empirical model is based on measurements that certainly used the IPS56 radiometric scale, hence the multiplication by a correction factor of 1.022 [33] to comply with the current WRR scale (whose announcement by the World Meteorological Organization in 1978 is posterior to the historical data used for the model's development).

G010. CLS

This is the Cloud Layer Sunshine model developed by Suckling and Hay [34,35]. Note that precipitable water must be in cm, contrarily to what is indicated in the original papers.

G011. CPCR2

This is the original CPCR2 model by Gueymard [36] with revised optical masses [3].

G012. Dogniaux

This combines the models that have been proposed by Dogniaux for direct radiation [37] and for diffuse radiation [38]. The expression for T_L as a function of β is taken here from [39]. See [25] for details.

G013. DPP

This is the Daneshyar–Paltridge–Proctor model tested in [4,40] and also reviewed in [41]. The DPP acronym is from Badescu [4]. The direct irradiance at normal incidence is here from the original paper by Daneshyar [42] who used the model of Paltridge and Proctor [43], with corrected unit for Z. (It is actually degrees rather than radians as Badescu or Daneshyar suggested.) Coefficients for diffuse irradiance are given by Daneshyar as 0.218 and 0.299 cal/(cm^2 h) for the USA, as cited from [44]. Daneshyar also suggests 0.123 and 0.181 for Iran. However, their Eq. (5a) suggests that Z is in radians, which is not correct. Goswami and Klett [40] used the USA values, which are used here too, after conversion from cal/(cm^2 h) to W/m^2. They used the correct unit for Z. Festa and Ratto [41] mention the Iran values, but with Z in radians rather than degrees, due to the confusion in the original papers. Badescu [4] also used radians, but with considerably larger values for the coefficients. To avoid further confusion, the modified equations as used here are provided below:

$$E_{bn} = 950[1 - \exp(-0.075h)] \tag{2}$$

$$E_d = 2.534 + 3.475h \tag{3}$$

Here E_{bn} and E_d stand for direct normal irradiance and diffuse irradiance, respectively, both measured in W/m^2. The sun altitude angle is given by $h = 90 - Z$ where Z is in degrees.

G014. ESRA1

This is the model that was used to develop the European Solar Radiation Atlas, with the broadband transmittances and turbidity computed according to Rigollier et al. [45,46]. Here the Linke turbidity coefficient for an air mass of 2 is obtained from the new Page's formula, Eq. (19) of [47]. This revision was suggested in [48]. For more details, see [10].

G015. ESRA2

This model is the same as ESRA1, except that T_L is now obtained using formulae proposed in [7,49].

G016. ESRA3

This model is similar to ESRA1 or ESRA2, but T_L is obtained from the empirical formula of [50] as a function of precipitable water and Angstrom's β coefficient.

G017. ESRA4

This model is again similar to ESRA1, but T_L is obtained here from Eq. (1).

G018. HLJ

This is the broadband model developed by Hottel [51] for direct irradiance, and later modified in [52–56], who all added the diffuse transmittance formula of Liu and Jordan [57], based on Hottel's own recommendation. The Hottel equations corresponding to a visibility of 23 km are used here, which is consistent with the literature cited. For more details, see [10].

G019. Ideriah

This model is proposed in Ideriah [58] based on the direct irradiance model by King and Buckius (see entry G027 below).

G020. Ineichen

This model comes from Ineichen's parameterization of the SOLIS spectral model [59]. For more details, see [10].

G021. Iqbal A

This is "model A" from Iqbal [33]. It is adapted from the McMaster (MAC) model [60]. The original formulation for the Rayleigh transmittance is used here, rather than Iqbal's Eq. (7.4.8), which contains a typo. For more details, see Gueymard [3,10].

G022. Iqbal B

This is "model B" from Iqbal [33]. It is adapted from the Hoyt model [61]. For more details, see [3,10].

G023. Iqbal C

This is "model C" from Iqbal [33]. It is adapted from Bird's model (entry G005 above). For more details, see [3,10,25].

G024. Josefsson

This is the model by Josefsson [62], as described, used and/or modified in [1,2]. See [3] for details.

G025. KASM

This is the modified Kasten model [63] according to [4].

G026. Kasten

This is another modification of the original Kasten model [63], this time following [2,64]. T_L is obtained from Eq. (1).

G027. King

This model uses the broadband transmittances and turbidity functions according to King and Buckius [19] and Buckius and King [65]. The former reference provides and expression that can be used to calculate direct irradiance [25]. In the latter reference, the diffuse irradiance is to be calculated from its Eq. (36), but two free parameters remain, namely κ_L and a_1. For this investigation, the function κ_L has been fitted to the numerical values provided in [65] for five discrete values of β, such as

$$\kappa_L = 0.8336 + 0.17257\beta - 0.64595\,\exp(-7.4296\beta^{1.5}) \tag{4}$$

Similarly, the value of coefficient a_1 was only described as varying between 0 and 1. The average value $a_1 = 0.5$ is assumed here in the absence of more specific indications.

G028. KZHW

This model was proposed by Krarti et al. [64] as a combination of those of Zhang and Huang [66] for global radiation and

Watanabe et al. [67] for the direct/diffuse component separation. The empirical coefficients as modified in [64] are used here.

G029. MAC

The McMaster model of Davies et al. [60] was later used and/or modified in [1,2,68]. The formulation (particularly for the Rayleigh and aerosol transmittances) used here is as described in [1]. A corrected Rayleigh transmittance expression is used here since it was misprinted in the latter report. For more details, see [3,10].

G030. Machler

This is the model proposed by Machler and Iqbal [69].

G031. METSTAT

This is a modified version of Bird's model (entry G007 above) according to Maxwell [70]. For more details, and how to evaluate the Unsworth–Monteith turbidity coefficient it uses, see [3,10,25].

G032. MRM4

This model is described by Muneer et al. [71] and Kambezidis [72]. The numerical coefficients considered here are for the USA and southern Europe, as given in [73, p. 73]. For more details, and a discussion of this model's shortcomings, see [25,74].

G033. MRM5

More than a mere revision of MRM4 (entry G032 just above), this is actually a completely different algorithm. It is adapted here from Fortran code, version 5, by Kambezidis and Psiloglou [75,76]. Ozone, precipitable water, Angstrom's coefficient β and albedo are the input variables here, as discussed in [10].

G034. Nijegorodov

This model [77] uses the air mass formula from Nijegorodov and Luhanga [78] and transmittance expressions from Bird's model (entry G007 above). It is assumed here that the Earth radius is 6367 km and that the effective atmosphere thickness is 29.7 km.

G035. NRCC

The original model by Belcher and DeGaetano [79,80] was slightly modified according to personal communications with Belcher [81], as discussed in [10].

G036. Paltridge

This is the empirical model of Paltridge and Platt [82].

G037. Perrin

This is the broadband model of Perrin de Brichambaut and Vauge [83], as discussed in [25].

G038. PR

A part of this model is described in Psiloglou et al. [84]. However, the aerosol transmittance expression is here from the REST model [25] per Psiloglou's request [85], with the purpose to improve the model's performance. The new acronym stands for "Psiloglou-REST".

G039. PSIM

This model is described by Gueymard [74] and its performance for direct irradiance predictions was discussed in [25,74].

G040. REST250

This is version 5.0 of the REST2 model, as described by Gueymard [86].

G041. Rodgers

This model uses the Unsworth–Monteith turbidity coefficient. It is described by Rodgers et al. [87]. See also [25].

G042. RSC

Carroll [88] combined earlier algorithms by Robinson [89] and Sellers [90] to derive this model, hence its acronym.

G043. Santamouris

This model is based on atmospheric transmittances from Psiloglou et al. [84] (entry G029 above), following the advice of Dr. Santamouris [91]. A pressure correction was added where needed for consistency, as also discussed in [25].

G044. Schulze

This model was proposed by Schulze [92].

G045. Sharma

This empirical model was proposed by Sharma and Pal [93]. They used a solar constant of 2 cal/(cm^2 min), which is replaced here by the more recent value of 1366.1 W/m^2 [14].

G046. Watt

This model was proposed by Watt [94], and its performance was studied by Bird and Hulstrom [24]. These authors, however, seem to have misinterpreted some equations, due to Watt's non-explicit use of the decimal logarithm. This can explain the subpar performance results of the Bird and Hulstrom study. The required extinction layer heights are derived here from the original author's Fig. 4.0.2. A fixed stratospheric turbidity of 0.02 is assumed.

G047. Wesely

This model by Wesely and Lipschutz [95,96] uses visibility, which is derived here from Angstrom's β coefficient by using the formula of [19] in reverse mode.

G048. Yang

The original model of Yang et al. [97] is used here with the corrections described in [25], which were eventually included in a later description of the model [98].

G049. Zhang

The model proposed by Zhang et al. [66,99] described site-specific coefficients empirically derived from radiation measurements in China. For this study, the average of the coefficients tabulated for 24 sites [99] was rather used for improved universality. The model's Gompertz function that separates the direct and diffuse components appeared to generate unphysical values, which was caused by its coefficient a_4 being misprinted. The correct value (2.99) is used here [100].

G050. HS

This is a combination between the model by Haurwith [101,102] to predict direct irradiance and the model by Schulze [92] to predict diffuse irradiance.

G051. ABCGS

This is a combination between the model by Adnot–Bourges–Campana–Gicquel [103] to predict direct irradiance and the model by Schulze [92] to predict diffuse irradiance.

G052. Paulescu and Schlett

In this model by Paulescu and Schlett [104], the value $\gamma = 0.5$ is adopted here to approximate a Rayleigh atmosphere, based on the suggestion by Paulescu [105].

G053. Janjai

This model is based on publications by Janjai [106] and Janjai and Sricharoen [107].

G054. REST281

This is version 8.1 of REST2 model, which contains a few corrections compared to the entry G040 above and the original description by Gueymard [86]. For more details on this model see Gueymard [10].

3. Input data

The input data depends on model. Table 1 shows the input parameters needed by all models while Table 2 shows the entries needed by each model. The input data have been organized in several databases as described next.

3.1. Solar radiation measurements

The solar radiation database consists of global and diffuse hourly irradiation measured by using Kipp & Zonen radiometers in Cluj-Napoca and Bucharest-Afumati (see Table 3 for geographic coordinates). A Kipp & Zonen CM11 device is operating at Bucharest-Afumati station while the Cluj-Napoca station is provided with CM6B devices. The measurement uncertainty is ±3% for

Table 1
Input data for models used in this work.

Symbol	Meaning
Astronomical	
Year	Number of year
Month	Number of the month in the year (1 to 12)
Day	Number of day in the month (1 to 31)
h	Hour (UTC)
δ	Sun declination (deg.)
z	Zenith angle (deg.)
E_{sc}	Solar constant (W/m^2)
E_{n0}	Extraterrestrial irradiance (W/m^2), corrected for the actual sun-earth distance
m_K	Kasten's air mass
m_{KY}	Kasten & Young's air mass
Geographical	
λ	Latitude (deg)
φ	Longitude (deg)
h_g	Site's elevation (meter)
ρ_g	Ground albedo
Meteorological (surface)	
p	Surface air pressure (hPa)
T	Air temperature, dry-bulb (K)
ΔT	dry-bulb temperature T at time t, $T(t)$, $-T(t-3\,h)$
U	Surface air relative humidity (%)
W	Wind speed (m/s)
Meterological (column integrated)	
u_o	Reduced ozone vertical pathlength (atm-cm)
u_N	Total NO_2 vertical pathlength (atm-cm)
w	Precipitable water (cm)
Quantities related to atmospheric turbidity	
α	Angstrom wavelength exponent
β	Angstrom turbidity
α_1	Angstrom wavelength exponent for <700 nm
α_2	Angstrom wavelength exponent for >700 nm
ϖ_1	Aerosol single-scattering albedo, <700 nm
ϖ_2	Aerosol single-scattering albedo, >700 nm
T_{L1}	Linke turbidity estimated by using Page/Remund method [47]
T_{L2}	Linke turbidity estimated by using Ineichen method [7]
T_{L3}	Linke turbidity estimated from the empirical formula of Dogniaux [50] as a function of precipitable water and Angstrom's beta coefficient
T_{L4}	Linke turbidity estimated from the average of four linear relationships between Angstrom's beta coefficient and Linke turbidity by Hinzpeter [29], Katz et al. [30], Abdelrahman et al. [31] and Grenier et al. [32].
τ_a	Unsworth–Monteith broadband turbidity coefficient
τ_{700}	Aerosol optical depth at 700 nm, dimensionless
vis	Visibility (km)

CM11 and ±5% for CM6B. The temperature dependence of sensitivity is ±1% for CM11 and ±2% for CM6B, on the interval −20 to +40 °C. On a monthly basis the bias for CM6B ranges between −2% and +0.9% [108]. The radiometers are checked twice per week and cleaned when necessary.

The measurement methodology is provided by standard procedures prepared at the Romanian National Meteorological Administration. Measurements are performed as follows. Solar irradiance (units: W/m^2) is measured at 1-min intervals. The series of irradiance values are averaged over 10 min, 60 min and 1440 min, respectively. Irradiation values (units: J) for 10 min, 1 h and 24 h are obtained by multiplying the appropriate average irradiance values by the appropriate time duration. The integration interval starts ½ hour before the time stamp in the files and ends ½ hour after that time stamp. Central European Time is used in the files.

The radiometers are calibrated once per year through shaded–unshaded measurements in clear sky days and through direct irradiance measurements on a horizontal surface with reference to the Linke-Feussner etalon actinometer. The Linke-Feussner etalon is calibrated with reference to the national etalon, i.e. an Angstrom 702 pirheliometer with electric compensation. The national etalon is calibrated once at five years with reference to the World Radiometric Reference at Davos (Swiss).

Partial sky obstructions or shading of the sensors by natural or artificial structures is low and is not considered. There are less than 0.1% missing or suspicious data.

3.2. Surface meteorological data

Meteorological data measured in all stations of Table 3 are used in this study. A few details follow. In case of Bucharest, some of the meteorological variables are measured at Bucharest-Baneasa station, whereas other parameters are measured at Bucharest-Afumati station. Sunshine duration is calculated from solar radiation by using the World Meteorological Organization sunshine criterion [109]. This stipulates that the "sun is shining" if the global solar irradiance measured perpendicular on sun's rays exceeds 120 W/m^2. Sunshine data are recorded hourly. Daily totals are also computed. Measurements are reported in tens of an hour.

3.3. Column integrated data

3.3.1. Ozone

Long-term measurements of column-integrated ozone are performed in Romania once per day at a single station (Bucharest-Baneasa). Measurements are performed usually in the interval 0900–1400 (Eastern European Time). There are missing days in the recordings (Saturdays, Sundays as well as other days). The WOUDC archive provides data for Bucharest during 1980–2006. Ozone data measured in 2009 are used here (see Fig. S1 of [11]).

3.3.2. Precipitable water

Data for column-integrated precipitable water are available from two stations. Radiosonde measurements are performed twice daily at Bucharest-Baneasa (0000 and 1200 UTC) and once daily at Cluj-Napoca (0000 UTC). Daily measurements for precipitable water performed during 2009 at Cluj-Napoca and Bucharest-Baneasa (see Figs. S2 and S3 in [11]).

3.4. Satellite derived data

3.4.1. Surface albedo

The ground albedo is obtained for all stations from satellite images on a monthly basis and 15-km spatial resolution. We have used the Surface Albedo (SAL) product of the Satellite Applications Facility on Climate Monitoring (CM-SAF) (http://www.cmsaf.eu), which is part of the EUMETSAT distributed ground segment. The product line covers broadband albedo products from the SEVIRI instrument aboard Meteosat-9 [110]. No information about topography or terrain roughness around the weather stations was included in the input data files at this stage. Figs. S4 and S5 of [11] show monthly albedo information for Cluj-Napoca and Bucharest-Baneasa, respectively, as observed during 2009.

3.4.2. Atmospheric turbidity data

For each station under scrutiny, the Ångström turbidity coefficients α and β, as well as the aerosol single-scattering albedo ϖ, are obtained from world datasets [111]. These are climatological (long-term monthly average) values, whereas daily values would ideally be necessary. These datasets actually provide the aerosol optical depth at 550 nm, τ_{a550}, rather than β. The latter must therefore be calculated from Ångström's Law:

$$\beta = \tau_{a550} \cdot 0.55^{\alpha} \tag{5}$$

Data files containing values of α, τ_{a550} and ϖ are the primary databases that are used here to evaluate aerosol extinction in those models that take it into account. Data is gridded at 1 × 1° resolution,

Table 2
Input data for tested models.

Model number	Model name	z	m	ρ_g	p	T	U	W	vis	w	u_o	u_n	α	β	τ_a	T_L	ϖ
G001	ASHRAE72	X															
G002	ASHRAE05	X															
G003	Badescu	X	X		X					X	X						
G004	Bashasu	X	X		X					X				X			
G005	BCLSM	X	X							X							
G006	Biga	X															
G007	Bird	X	X	X	X					X	X		X	X			
G008	CEM	X		X	X					X					X		
G009	Chandra	X														X	
G010	CLS	X	X	X	X					X							
G011	CPCR2	X		X	X					X	X		X	X			X
G012	Dognio	X	X		X											X	
G013	DPPLT	X															
G014	ESRA1	X	X		X											X	
G015	ESRA2	X	X		X											X	
G016	ESRA3	X	X		X											X	
G017	ESRA4	X	X		X											X	
G018	HLJ	X															
G019	Ideria	X	X		X					X			X	X			
G020	Ineich	X			X					X					X		
G021	IqbalA	X	X	X	X	X				X	X		X	X			
G022	IqbalB	X	X	X	X	X				X	X			X			
G023	IqbalC	X	X	X	X	X				X	X		X	X			
G024	Josefs	X	X	X	X					X							
G025	KASM	X	X		X					X							
G026	Kasten	X	X		X											X	
G027	King	X	X	X	X					X				X			
G028	KZHW	X				X	X	X									
G029	MAC	X		X	X	X				X							
G030	Machler	X			X				X	X							
G031	METSTAT	X	X	X	X					X	X				X		
G032	MRM4	X	X		X					X	X						
G033	MRM5	X	X	X	X					X	X			X			
G034	Nijego	X	X		X	X				X	X		X	X			
G035	NRCC	X			X		X		X	X							
G036	Paltri	X															
G037	Perrin	X	X		X					X	X			X			
G038	PR	X	X	X	X					X	X			X			
G039	PSIM	X		X	X					X				X			
G040	REST250	X		X	X					X	X	X	X	X			X
G041	Rodger	X			X					X					X		
G042	RSC	X	X	X	X					X				X			
G043	Santa	X	X	X	X					X	X						
G044	Schulz	X															
G045	Sharma	X															
G046	Watt	X	X	X	X					X	X		X	X			
G047	WKB	X	X		X				X								
G048	Yang	X	X		X					X	X			X			
G049	Zhang	X				X	X										
G050	HS	X															
G051	ABCGS	X															
G052	Paulescu	X	X		X					X	X			X			
G053	Janjai	X	X		X					X	X		X	X			
G054	REST281	X		X	X					X	X	X	X	X			X

Table 3
Meteorological stations involved in this study.

Geographic Code	Station	Latitude (deg N)	Longitude (deg E)	Altitude (m)
430613	Bucharest-Afumati	44.50	26.21	90
430608	Bucharest-Baneasa	44.50	26.13	90
647334	Cluj-Napoca	46.78	23.57	417

and no correction for elevation is considered. Ideally, a much finer spatial resolution (such as 10 km × 10 km) would be necessary for validation purposes, but this is currently not available. Figs. S4 and S5 in [11] show the monthly values of α, τ_{550} and ϖ at Cluj-Napoca and Bucharest-Baneasa, respectively. Since no information about the inputs $\alpha_1, \alpha_2, \varpi_1$ and ϖ_2 in models G040 and G054 is available, the following approximations are used:

$$\alpha_1 = \alpha_2 = \alpha \tag{6}$$

$$\varpi_1 = \varpi_2 = \varpi \tag{7}$$

The monthly data were smoothed to derive daily data.

3.5. Default values

The column-integrated nitrogen dioxide content is not measured. Constant values of 0.0002 atm cm over rural areas and

0.0005 atm cm over cities are assumed. The latter value is adopted here for both Bucharest and Cluj-Napoca.

4. Testing procedure

4.1. Compatibility between various input datasets

Since the input datasets come from various sources, it is important to check their compatibility.

4.1.1. Spatial compatibility of measurement datasets at Bucharest

Bucharest has three main meteorological stations, two of them being of importance here: Bucharest-Baneasa and Bucharest-Afumati. Most meteorological data used as input for testing the models at Bucharest are measured at Bucharest-Baneasa. However, the sunshine data come from Bucharest-Afumati. The two stations are 10.8 km away (see Fig. S6 of [11]). Although the relative sunshine might be different at the two stations, the testing procedure used here refers to clear days only. It is likely that the sky will be clear simultaneously at both stations, considering the short distance and homogeneous terrain. The same should be true for the meteorological variables measured at one station and used to model solar radiation at the other. Therefore it is anticipated that the distance issue will not significantly affect the results.

4.1.2. Time compatibility between measurements datasets

Most meteorological datasets are prepared with reference to UTC. Solar radiation datasets and relative sunshine are reported by using Central European Time. Time compatibility has been ensured between different datasets. We used different procedures to obtain time integrations of various quantities (such as relative sunshine and solar irradiation). A preprocessing of the data was therefore needed before it could be used for this study. The quantities were grouped according to their measurement time stamp and two or more files with input data were prepared for the same station; each file contains those measured quantities associated to the same measurement time.

4.1.3. Compatibility between datasets

Disagreement may exist between the two quantities related to the state of the sky: cloud cover amount C and relative sunshine σ (both quantities range between 0 and 1). Indeed, the cloud cover amount is an instantaneous quantity while the relative sunshine results by time integration. The sky might be clear at the estimation moment (hence $C=0$) while during the integration interval the sun may be covered by clouds from time to time, resulting a $\sigma<1$ relative sunshine value. However, at Bucharest the disagreement between C and σ may be larger than usual because these two quantities are measured in two different locations.

4.2. Computation of various quantities

4.2.1. Astronomical quantities

Irradiance is a strong function of the solar zenith angle, Z. Most models take the solar geometry into account through the relative air mass, m, rather than Z. The specific relationship between m and Z recommended by each model is used here. Computations were performed only for $Z<85^\circ$ to avoid inaccuracies resulting from possible horizon shading or experimental cosine errors, for instance.

4.2.2. Atmospheric turbidity parameters

A more elaborate value of the Angstrom turbidity coefficient β is used in computation. A first estimate of the Angstrom turbidity (say $\hat{\beta}$) is computed by using Eq. (5). Next, the modal value β is calculated from

$$\beta = \frac{\hat{\beta}(0.83212 + 3.2104\hat{\beta})}{1 + 5.852\hat{\beta}^{0.75}} \tag{8}$$

Some models use a special value of β that corresponds to an α value fixed at 1.3. It is calculated here by using Eq. (5) with $\alpha = 1.3$. These various inputs used by different models to evaluate the effects of aerosols are shown in Table 2. No elevation correction is needed since all locations are low altitude.

The parameter β_2 for models G040 and G054 corresponds to α determined from spectral measurements of aerosol optical depth (AOD) for wavelengths between 700 and 1000 nm. Since no information about β_2 is available, the following approximation is used:

$$\beta_2 = \beta \tag{9}$$

A simplified way of characterizing the optical depth of aerosols is through a broadband turbidity index. Well-known examples of such are the Linke turbidity factor, T_L, and the broadband aerosol optical depth (BAOD), τ_a, also known as the Unsworth–Monteith coefficient. These indicators are input for some models as shown in Table 2.

4.3. Accuracy indicators

One considers n couples of measured and computed values, denoted m_i and c_i ($i=1,n$), respectively. The mean values of these measured and computed values are defined as:

$$\bar{m} \equiv \frac{1}{n}\sum_{i=1}^{n} m_i \tag{10}$$

$$\bar{c} = \frac{1}{n}\sum_{i=1}^{n} c_i \tag{11}$$

For the ith couple, the difference between the predicted and the measured value is:

$$e_i \equiv c_i - m_i \tag{12}$$

Note that this difference e_i has the same physical dimension as m_i and c_i. This difference would be an error if m_i could be considered the truth, which is obviously not the case, since all measurements have their own uncertainty.

The most common bulk performance statistics are the Mean Bias Error (*MBE*) and the Root Mean Square Error (*RMSE*) which are defined as

$$MBE = \frac{1}{n\bar{m}}\sum_{i=1}^{n} e_i \tag{13}$$

$$RMSE = \frac{1}{\bar{m}}\sqrt{\frac{1}{n}\sum_{i=1}^{n} e_i^2} \tag{14}$$

Eqs. (13) and (14) provide dimensionless quantities since their right hand side has been divided by the mean measured irradiance or irradiation. In what follows, they are expressed in percent for clarity.

4.4. Broad criteria for model performance

A model designed to compute hourly solar irradiation provides good performance if the MBE and RMSE have as low values as possible. The following quantitative recommendations are sometimes used [9]. For global irradiation, MBE within ±10% and RMSE < 20% indicate good fitting between model results and measurements.

For diffuse irradiation, a good fitting means MBE within ±20% and RMSE < 30%.

Here more stringent criteria for model performance are adopted. A model to compute solar *global* hourly irradiation provides "good performance" if:

- the model is well calibrated (i.e. −5% < MBE < +5%) and
- the scatter in the results is such that RMSE < 15%.

A model to compute solar *diffuse* hourly irradiation provides "good performance" if:

- it is well calibrated (i.e. −10% < MBE < +10% and
- the scatter in the results is such that RMSE < 30%).

5. Results and discussion

In the following we denote by σ the hourly relative sunshine (between 0 and 1) and by C the total cloud cover amount (between 0 and 1 – instantaneous quantity).

The testing procedure is performed in several stages intended to provide information about the sensitivity of the models to various sets of input data. Separate analyses are performed for Cluj-Napoca and Bucharest. In both cases, details are first provided about the available input data while the results are reported next. Finally, an overall conclusion about models' performance is drawn.

5.1. Analysis for Cluj-Napoca

A first test (so called Stage 1) consisted of checking the procedure. A large number of subsequent tests have been performed for Cluj-Napoca by using data from 2009. The most relevant steps are reported here.

5.1.1. Input data

Stage 2

This testing stage is associated to the best available input data. Only data associated to $C = 0$ and $\sigma = 1$ were used. A total of 133 hourly recordings were used in calculations.

Daily measurements for precipitable water performed once per day at 0.00 UTC at Cluj-Napoca were used. Daily measurements for ozone performed once per day at 12.00 UTC at Bucharest were used for Cluj-Napoca. For intermediate hours, precipitable water and ozone values were linearly interpolated between two consecutive measured values. Satellite data were used to derive monthly averaged values for albedo, α, τ_{550} and ϖ for Cluj-Napoca. Each value derived from satellite data was associated to the 15th day in a month. For intermediate days, values were linearly interpolated. A constant value is assumed during the day.

Stage 3

This testing stage estimates models performance sensitivity to input data related to visual (direct) estimation of the state of the sky. Therefore, only data associated to $C = 0$ were used while the values of σ are free to vary. A few data points associated to $C = 0$ and $\sigma = 0$ exist. They may occur in clear days near the sunrise and sunset, when the global radiation is small and the WMO "sun shining" criterion may not work. Other input data are similar to those for Stage 2. A total of 166 hourly recordings were used in calculations.

Stage 4

This testing stage estimates models performance sensitivity to input data related to (indirect) estimation of the state of the sky (i.e. by means of sunshine recordings). Indeed, the approximation $C = 1 - \sigma$ is sometimes used in literature when data on cloud cover amount is missing. Only data associated to $\sigma = 1$ were used while the values of C are free to vary. Many of the cloud cover values equal 0, as expected. However, positive values of C are also present. Such sort of situations may be imagined. Indeed, the sun may shine continuously for 1 h despite some parts of the sky being covered by clouds. Other input data are similar to those used for Stage 2. A total of 775 hourly recordings were used in calculations.

Stage 5

This testing stage estimates models performance sensitivity to input data related to ozone content in the atmosphere. A constant value $u_o = 0.3$ atm cm was assumed all over the year. Other input data are similar to those of Stage 2. A total of 133 hourly recordings were used in calculations.

Stage 6

This testing stage estimates models performance sensitivity to input data related to precipitable water. The precipitable water content has been computed by using Leckner formula [112]. Other input data are similar to those used for Stage 2. A total of 133 hourly recordings were used in calculations.

Stage 7

This testing stage estimates models performance sensitivity to input data related to ground albedo. A constant value 0.2 has been used for the ground albedo all over the year. Other input data are similar to those used for Stage 2. A total of 133 hourly recordings were used in calculations.

Stage 8

This testing stage estimates models performance sensitivity to input data related to visual estimation of the state of the sky *and* ozone. Only data for $C = 0$ were used (i.e. the values of the sunshine fraction are free to vary). Other input data are similar to those used for Stage 5 (where a constant ozone value has been used as input). A total of 166 hourly recordings were used in calculations.

Stage 9

This testing stage estimates models performance sensitivity to input data related to visual estimation of the state of the sky *and* precipitable water. Only data for $C = 0$ were used (i.e. the values of the sunshine fraction are free to vary). Other input data are similar to those used for Stage 6 (where the precipitable water has been computed by using Leckner's formula [112]). A total of 166 hourly recordings were used in calculations.

Stage 10

This testing stage estimates models performance sensitivity to input data related to visual estimation of the state of the sky *and* ground albedo. Only data for $C = 0$ were used (i.e. the values of the sunshine fraction are free to vary). Other input data are similar to those used for Stage 7 (when a fixed value of ground albedo has been used). A total of 166 hourly recordings were used in calculations.

Stage 11

This testing stage estimates models performance sensitivity when measurements about ozone, precipitable water and ground albedo are missing but surface measurement data are available. A constant ozone amount 0.3 atm cm has been assumed. Precipitable water has been computed by using Leckner formula [112]. A constant ground albedo value (0.2) has been assumed. Other input data are similar to those used for Stage 2. A total of 133 hourly recordings were used in calculations.

Stage 12

This testing stage estimates models performance sensitivity when measurements about ozone, precipitable water and ground albedo are missing and only visual information about the state of the sky exists. Only data for $C = 0$ were used (i.e. the values of the sunshine fraction are free to vary). Other input data are similar to those used for Stage 11. A total of 166 hourly recordings were used in calculations.

Stage 13

This testing stage is associated to the best available input data during the extended warm season (April–October). Only data associated to $C = 0$ and $\sigma = 1$ were used. Other input data are similar to

those used for Stage 2. A total of 129 hourly recordings were used in calculations.

Stage 14

This testing stage is associated to the best available input data during the extended cold season (November–March). Only data associated to $C = 0$ and $\sigma = 1$ were used. Other input data are similar to those used for Stage 2. A total of 4 hourly recordings were used. Therefore, the results associated to this Stage should be taken with caution due to the small number of recordings.

Stage 15

This testing stage estimates models performance sensitivity during the extended warm season (April–October) to input data related to visual estimation of the state of the sky. Therefore, only data associated to $C = 0$ were used while the values of σ are free to vary. Other input data are similar to those used for Stage 3. A total of 161 hourly recordings were used.

Stage 16

This testing stage estimates models performance sensitivity during the extended cold season (November–March) to input data related to visual estimation of the state of the sky. Therefore, only data associated to $C = 0$ were used while the values of σ are free to vary. Other input data are similar to those used for Stage 3. A total of 5 hourly recordings were used.

Stage 17

This testing stage estimates models performance sensitivity during the extended warm season (April–October) to input data related to indirect estimation of the state of the sky. Only data associated to $\sigma = 1$ were used in this stage while the values of C are free to vary. Other input data are similar to those used for Stage 4. A total of 695 hourly recordings were used in calculations.

Stage 18

This testing stage estimates models performance sensitivity during the extended cold season (November–March) to input data related to indirect estimation of the state of the sky. Only data associated to $\sigma = 1$ were used in this stage while the values of C are free to vary. Other input data are similar to those used for Stage 4. A total of 65 hourly recordings were used in calculations.

Stage 19

This testing stage estimates models performance sensitivity when measurements about ozone, precipitable water and ground albedo are missing but surface measurement data are available for the extended warm season (April–October). Other input data are similar to those used for Stage 11. A total of 129 hourly recordings were used in calculations.

Stage 20

This testing stage estimates models performance sensitivity when measurements about ozone, precipitable water and ground albedo are missing but surface measurement data are available during the extended cold season (November–March). Other input data are similar to those used for Stage 11. A total of 4 hourly recordings were used in calculations.

Stage 21

This testing stage estimates models performance sensitivity during the extended warm season (April–October) when measurements about ozone, precipitable water and ground albedo are missing but visual information about the state of the sky is available. Only data for $C = 0$ were used (i.e. the values of the sunshine fraction are free to vary). Other input data are similar to those used for Stage 12. A total of 161 hourly recordings were used in calculations.

Stage 22

This testing stage estimates models performance sensitivity during the extended cold season (November–March) when measurements about ozone, precipitable water and ground albedo are missing but visual information about the state of the sky is available. Only data for $C = 0$ were used (i.e. the values of the sunshine fraction are free to vary). Other input data are similar to those used for Stage 12. A total of 5 hourly recordings were used in calculations.

5.1.2. Results

Table 4 shows the models accuracy for computing global radiation at Cluj-Napoca. MBE is used as the main accuracy indicator. No model passed the testing stages 4, 17 and 18. This is not surprising since the catalogue contains clear sky models only and such sort of models has no input parameter associated to the state of the sky. Despite the filter $\sigma = 1$ is imposed, the testing stages 4, 17 and 18 allow input data from days with cloudy sky (i.e. $C \neq 0$). Indeed, the sun may shine without intermittency for a whole hour, with some parts of the sky being covered by clouds.

Very simple clear sky models are defined as models which do not require meteorological data as input. Their input consists just of astronomic data. These models are G001, G002, G006, G013, G018, GC36, GC44, G045, G050, and G051 (see Table 2). Table 4 shows that very simple models as well as more complex models may belong to the category of "good models". This is in agreement with previous knowledge about the performance of clear sky models to computing global irradiation [3,9,10].

Table 5 shows models stratification according to their accuracy for computing global radiation at Cluj-Napoca. The best models listed there fulfill the performance criteria for both MBE and RMSE. However, MBE is used for ranking the models. No very simple model is ranked among the first three best models in the stage testing. A single partial exception exists: model G006 is the second best in Stage 18. But the RMSE criterion is not fulfilled for this Stage 18, as already pointed out.

Most of the worst performing models have rather complex input data sets (GC47, GC19, GC30, G005, G028, G010, G049). Only two very simple models are ranked among the worst three models per stage (G013 and G050).

Fig. 1 shows the number of testing stages per model with accuracy criteria fulfilled for both MBE and RMSE indicators. This way of classification stratified the models in several groups and the first eleven best groups are shown in Fig. 1. Nine models belong to the first three best groups. One of these models (i.e. G001) is a very simple model.

Table 6 shows the models accuracy for computing diffuse radiation at Cluj-Napoca. Again, MBE is used as the main accuracy indicator. No model passed the testing stages 4, 17 and 18. This mimics the case of computing global radiation (Table 4). However, the number of "good" models is smaller in case of computing diffuse radiation than global radiation (compare Tables 6 and 4, respectively). Indeed, only fourteen models gave good performance when computing diffuse radiation. Model G029 performs the best for most testing stages.

Table 7 shows models stratification according to their accuracy for computing diffuse radiation at Cluj-Napoca. The best models listed there fulfill the performance criteria for both MBE and RMSE but MBE is used to rank the models. No single very simple model is ranked the first in the stage testing. Among the very simple models, G006 is ranked in the first three best for several testing stages. Also, G002 is ranked the third best for two testing stages. All the worst performing models have rather complex input data sets.

Fig. 2 shows the number of testing stages per model with accuracy criteria fulfilled for both MBE and RMSE indicators. This way of classification stratified the models in several groups and the first nine best groups are shown in Fig. 2. Twelve models belong to the first three best groups. Three of these models (i.e. G001, G002 and G006) are very simple models.

Table 4
Models' accuracy for computing solar global radiation at Cluj-Napoca.

Color	Meaning
green	Good models (criteria for both MBE and RMSE are fulfilled)
yellow	Best model according to MBE criterion; RMSE criterion is fulfilled
blue	Best model according to MBE criterion; RMSE criterion is not fulfilled
purple	Worst models according to MBE criterion

	Stages																				
Model	**2**	**3**	**4**	**5**	**6**	**7**	**8**	**9**	**10**	**11**	**12**	**13**	**14**	**15**	**16**	**17**	**18**	**19**	**20**	**21**	**22**
G001	green	green		green	green	green	green	green	green	green	green	green	green	green				green	green	green	
G002															green						green
G003	green	green		green	green	green	green	green	green	green	green	green		green				green		green	
G004								green			green		green		green				green	green	green
G005															green				green		green
G006	green	green		green	green	green	green	green	green	green	green	green		green				green		green	
G007	green	green		green	green	green	green	green	green	green	green	green	green	green	green				green	green	green
G008	green	green		green	green	green	green	green	green	green	green	green	green	green	green				green	green	green
G009	green	green		green	green	green	green	green	green	green	green	green		green				green		green	
G010																					
G011													green		green				green		yellow
G012								green			green		green		yellow				green	green	green
G013		grey											green		green				green		green
G014													yellow		green				yellow		green
G015													green		green				green		green
G016	green	green		green	green	green	green	green	green	green	green	green	green	green	green			green	green	green	green
G017	green	green		green	green	green	green	green	green	green	green			green						green	
G018	green	green		green	green	green	green	green	green	green	green	green		green				green		green	
G019	red	red	red	red	red	red	red	red	red	red	red	red		red		red		red		red	
G020	green	green		green	green	green	green	green	green	green	green	green	green	green	green			green	green	green	green
G021															green						green
G022															green						green
G023		green			green		green	green	green		green		green	green	green				green	green	green
G024		green			green		green	green	green	green	green		green	green	green			green	green	green	green
G025		green			green		green	green	green	green	green		green	green	green			green	green	green	
G026	green	green		green	green	green	green	green	green	green	green	green	green	green				green	green	green	
G027																					
G028			blue													blue					
G029															green						green
G030	green	green		green	green	green	green	green	green	green	green	green		green				green		green	
G031	green	green		green	green	green	green	green	green	green	green	green	green	green				green	green	green	
G032	green	yellow		green	green	green	yellow	yellow	yellow	green	yellow	green		green				green		yellow	
G033	green	green			green		green	green	green	green	green	green	green	green	green			green	green	green	green
G034													green		green				green		green
G035	green	green		green	green	green	green	green	green	green	green	green		green				green		green	
G036																					
G037													green		green				green		
G038		green			green		green	green	green	green	green		green	green	green			green	green	green	green
G039													green		green				green		green
G040								green			green		green		green				green	green	green
G041													green		green				green		green
G042	green	green		green	green	green	green		green	green		green		green			blue	green			
G043	green			green		green						green									
G044	green	green		green	green	green	green	green	green	green	green	green		green				green		green	
G045	green	green		green	green	green	green	green	green	green	green	green		green				green		green	
G046													green		green						green
G047													red		red		red		red		red
G048		green						green	green		green		green		green				green	green	green
G049	green			green	green	green				green		green						green			
G050																					
G051													green		green				green		green
G052	green	green		yellow	green	green	green	green	green	yellow	green	green	green	green				yellow	green	green	
G053	yellow	green		green	yellow	yellow	green	green	green	green	green	yellow		yellow				green		green	
G054	green	green		green	green	green	green	green	green	green	green	green	green	green	green			green	green	green	

Table 5
Models ranking according to their accuracy to compute global solar radiation at Cluj-Napoca. The best models fulfill the performance criteria for both MBE and RMSE except for models whose number is underlined, which do not fulfill the RMSE criterion.

Stage	Ranking – best models			Ranking – worst models		
	1st	2nd	3rd	52nd	53rd	54th
2	53	52	35	13	47	19
3	32	53	3	5	47	19
4	28	49	43	50	13	19
5	52	35	53	13	47	19
6	53	52	35	13	47	19
7	53	52	35	13	47	19
8	32	45	52	5	47	19
9	32	53	3	5	47	19
10	32	53	3	5	47	19
11	52	53	35	13	47	19
12	32	3	53	5	47	19
13	53	52	35	13	47	19
14	14	15	54	30	19	47
15	53	32	52	5	47	19
16	12	40	41	28	49	47
17	28	49	43	50	13	19
18	42	6	35	10	19	47
19	52	53	35	13	47	19
20	14	15	24	49	30	47
21	32	53	3	5	47	19
22	11	41	12	28	49	47

5.2. Analysis for Bucharest

A large number of test stages have been performed for Bucharest by using 2009 data. The most relevant stages are reported here.

5.2.1. Input data

Stage 32

This testing stage is similar in most aspects to Stage 2. The differences are as follows. The precipitable water has been measured at Bucharest-Baneasa at 0.00 and 12.00 UTC. Daily measurements for ozone were performed at Bucharest at 12.00 UTC. Monthly averaged values for albedo, α, τ_{550} and ϖ for Bucharest have been used. A total of 324 hourly recordings were used during the analysis.

Stage 33

This testing stage is similar in most aspects to Stage 3. Only data associated to $C = 0$ were used while the values of σ are free to vary. Other input data are similar to the input data used for Stage 32. A total of 391 hourly recordings were used in analysis.

Stage 34

This testing stage is similar in most aspects to Stage 4. Only data associated to $\sigma = 1$ were used in this stage while the values of C are free to vary. Other input data are similar to the input data used for Stage 32. A total of 908 hourly recordings were used in computation.

Stage 35

This testing stage is similar in most aspects to Stage 5. A constant value $u_o = 0.3$ atm cm was assumed all over the year. Other input data are similar to the input data used for Stage 32. A total of 324 hourly recordings were used in computation.

Stage 36

This testing stage is similar in most aspects to Stage 6. The precipitable water content has been computed by using Leckner formula [112]. Other input data are similar to the input data

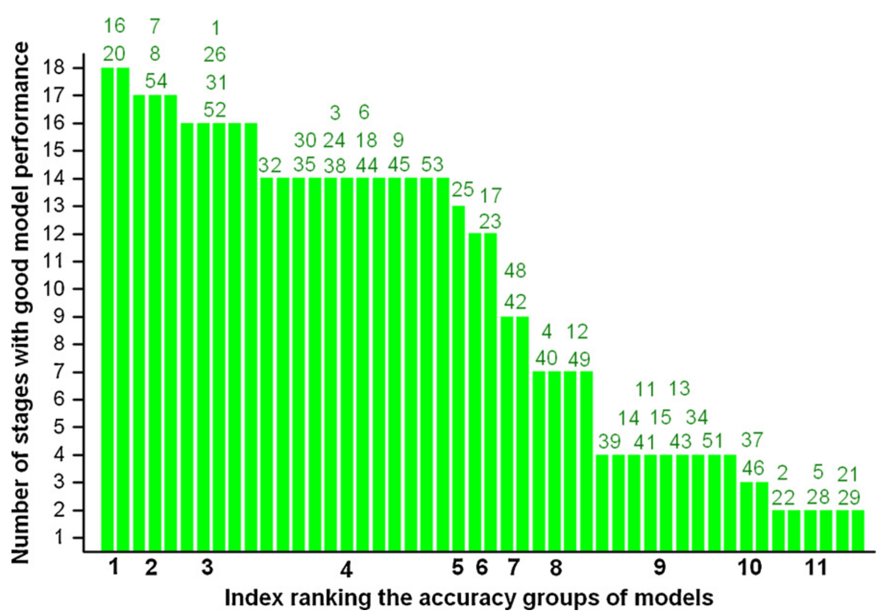


Fig. 1. Number of testing stages per model with accuracy criteria fulfilled for both MBE and RMSE indicators. The index ranking the accuracy groups of models is shown in ordinate. Global solar radiation at Cluj-Napoca is considered. The maximum number of testing stages is twenty-one.

Table 6
Models' accuracy for computing solar diffuse radiation at Cluj-Napoca.

Color	Meaning
green	Good models (criteria for both MBE and RMSE are fulfilled)
yellow	Best model according to MBE criterion; RMSE criterion is fulfilled
blue	Best model according to MBE criterion; RMSE criterion is not fulfilled
purple	Worst models according to MBE criterion

model	Stages 2	3	4	5	6	7	8	9	10	11	12	13	14	15	16	17	18	19	20	21	22
G001	green	green		green	green	green	green	green	green	green	green	green		green				green		green	
G002	green	green		green	green	green	green	green	green	green	green	green	green	green	green			green	green	green	green
G003																					
G004																					
G005																					
G006	green	green		green	green	green	green	green	green	green	green	green		green				green		green	
G007													green		green				green		green
G008																					
G009																	blue				
G010	green	green		green	green	green	green	green	green	green	green	green		green				green		green	
G011													green		green				green		green
G012	green			green	green	green	green	green		green	green	green						green		green	
G013																					
G014	green	green		green	green	green	green	green	green	green	green	green		green				green		green	
G015	green	green		green	green	green	green	green	green	green	green	green		green				green		green	
G016																					
G017													green		green				green		green
G018																					
G019	red	red	red	red	red	red	red	red	red	red	red	red		red		red		red		red	
G020	green	green		green	green	green	green	green	green	green	green	green		green				green		green	
G021													yellow		green				yellow		green
G022																					
G023													green		green				green		
G024						green												green			
G025													green		yellow				green		yellow
G026													green						green		
G027	green	green		green	green	green	green	green	green	green	green	green	green	green	green			green	green	green	green
G028																					
G029	yellow	yellow		yellow	yellow	yellow	yellow	yellow	yellow	yellow	yellow	yellow	green	yellow				yellow	green	yellow	
G030													red						red		
G031																					
G032																					
G033																					
G034			blue													blue					
G035																					
G036																					
G037																					
G038	green	green		green	green	green	green	green	green	green	green	green		green				green		green	
G039		green			green		green														
G040													green						green		
G041																					
G042																					red
G043																					
G044																					
G045	green			green	green	green				green		green		green				green		green	
G046																					
G047																					
G048																					
G049																					
G050																					
G051																					
G052	green	green		green	green	green	green	green	green	green	green	green		green				green		green	
G053															red		red				
G054	green	green		green	green	green	green	green	green	green	green	green		green				green		green	

used for Stage 32. A total of 324 hourly recordings were used in computation.

Stage 37

This testing stage is similar in most aspects to Stage 7. A constant value 0.2 this has been used for the ground albedo all over the year. Other input data are similar to the input data used for Stage 32. A total of 324 hourly recordings were used in computation.

Stage 38

This testing stage is similar in most aspects to Stage 8. Only data for $C = 0$ were used (i.e. the values of the sunshine fraction are free to vary). Other input data are similar to the input data used for Stage

Table 7
Models ranking according to their accuracy to compute diffuse solar radiation at Cluj-Napoca. The best models fulfill the performance criteria for both MBE and RMSE except for models whose number is underlined, which do not fulfill the RMSE criterion.

Stage	Ranking – best models			Ranking – worst models		
	1st	2nd	3rd	52nd	53rd	54th
2	29	6	$\underline{46}$	30	32	19
3	29	6	$\underline{5}$	30	32	19
4	$\underline{34}$	$\underline{3}$	$\underline{43}$	22	32	19
5	29	6	$\underline{46}$	30	32	19
6	29	6	52	30	32	19
7	29	6	$\underline{46}$	30	32	19
8	29	6	$\underline{5}$	30	32	19
9	29	6	54	30	32	19
10	29	6	$\underline{5}$	30	32	19
11	29	6	14	30	32	19
12	29	6	52	30	32	19
13	29	6	$\underline{46}$	30	32	19
14	21	27	2	42	53	30
15	29	6	$\underline{5}$	30	32	19
16	25	21	27	30	42	53
17	$\underline{34}$	$\underline{16}$	$\underline{3}$	22	32	19
18	$\underline{9}$	$\underline{43}$	$\underline{28}$	37	42	53
19	29	14	6	30	32	19
20	21	27	2	32	42	30
21	29	6	14	30	32	19
22	25	21	27	32	30	42

35 (i.e. with a constant ozone value as input). A total of 391 hourly recordings were used in computation.

Stage 39

This testing stage is similar in most aspects to Stage 9. Only data for $C = 0$ were used (i.e. the values of the sunshine fraction are free to vary). Other input data are similar to the input data used for Stage 36 (i.e. with precipitable water computed by using Leckner's formula [112]). A total of 391 hourly recordings were used in computation.

Stage 40

This testing stage is similar in most aspects to Stage 10. Only data for $C = 0$ were used (i.e. the values of the sunshine fraction are free to vary). Other input data are similar to the input data used for Stage 37 (i.e. with fixed value of ground albedo). A total of 391 hourly recordings were used in computation.

Stage 41

This testing stage is similar in most aspects to Stage 11. A constant ozone amount 0.3 atm cm has been assumed. Precipitable water has been computed by using Leckner formula [112]. A constant ground albedo value (0.2) has been assumed. Other input data are similar to the input data used for Stage 32. A total of 324 hourly recordings were used in computation.

Stage 42

This testing stage is similar in most aspects to Stage 12. Only data for $C = 0$ were used (i.e. the values of the sunshine fraction are free to vary). Other input data are similar to the input data used for Stage 41. A total of 391 hourly recordings were used in computation.

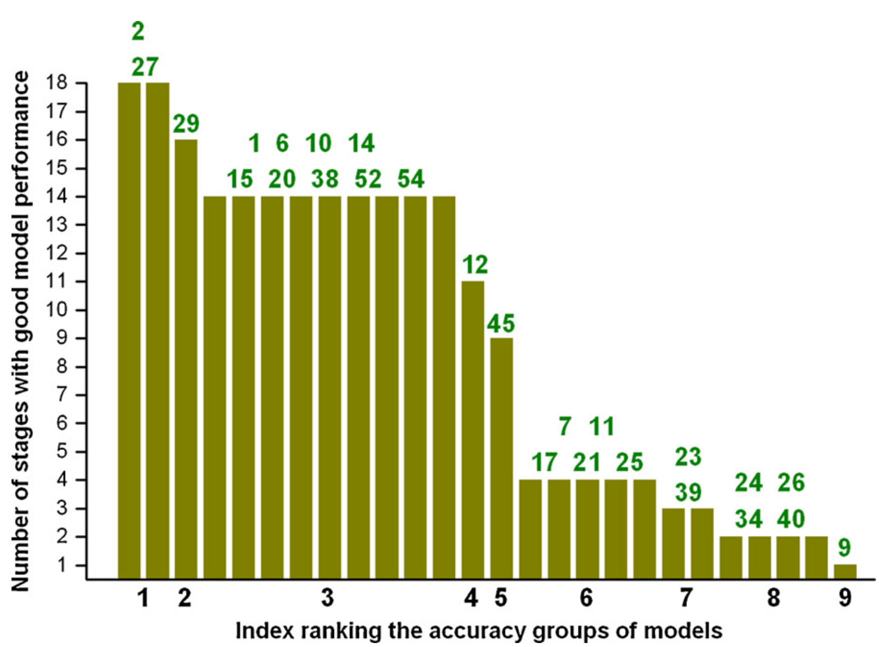
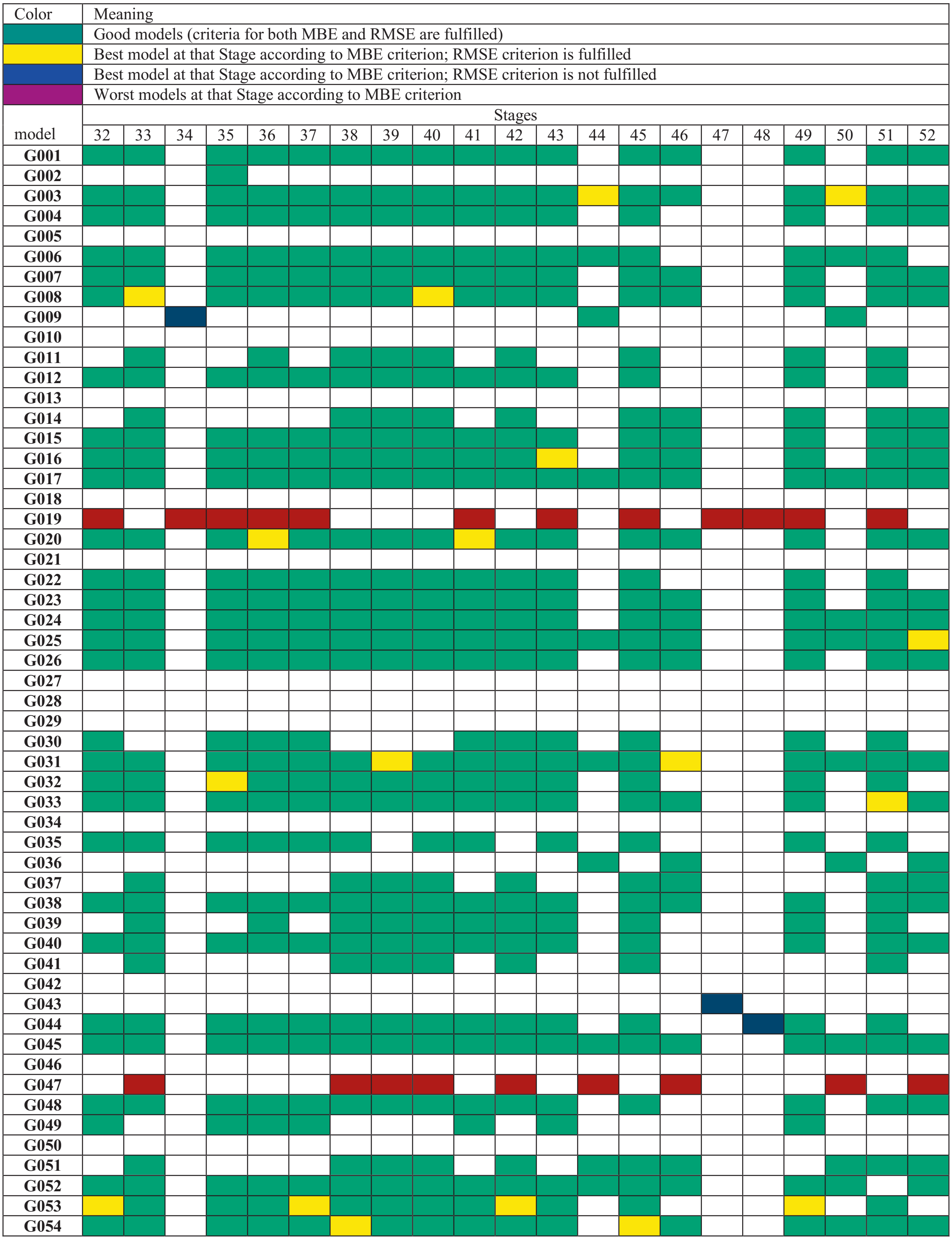


Fig. 2. Same as Fig. 1, for diffuse solar radiation at Cluj-Napoca.

Table 8
Models accuracy for computing solar global radiation at Bucharest.



Stage 43

This testing stage is similar in most aspects to Stage 13. Only data associated to $C = 0$ and $\sigma = 1$ were used. Other input data are similar to the input data used for Stage 32. A total of 289 hourly recordings were used in computation.

Stage 44

This testing stage is similar in most aspects to Stage 14. Only data associated to $C = 0$ and $\sigma = 1$ were used. Other input data are similar to the input data used for Stage 32. A total of 35 hourly recordings were used in computation.

Stage 45

This testing stage is similar in most aspects to Stage 15. Only data associated to $C = 0$ were used while the values of σ are free to vary. Other input data are similar to the input data used for Stage 33. A total of 328 hourly recordings were used in computation.

Table 9
Models ranking according to their accuracy to compute global solar radiation at Bucharest. The best models fulfill the performance criteria for both MBE and RMSE except for models whose number is underlined, which do not fulfill the RMSE criterion.

Stage	Ranking – best models			Ranking – worst models		
	1st	2nd	3rd	52nd	53rd	54th
32	53	3	32	13	47	19
33	8	54	45	5	19	47
34	9	42	43	5	47	19
35	32	3	16	13	47	19
36	20	16	32	5	47	19
37	53	3	32	13	47	19
38	54	8	45	5	19	47
39	31	33	45	5	19	47
40	8	54	45	5	19	47
41	20	16	32	5	47	19
42	53	45	17	5	19	47
43	16	3	30	13	47	19
44	3	45	52	30	19	47
45	54	33	17	5	47	19
46	31	25	36	30	19	47
47	43	42	18	5	13	19
48	44	30	43	50	47	19
49	53	30	8	5	47	19
50	3	52	45	30	19	47
51	33	31	38	5	47	19
52	25	31	54	19	30	47

Stage 46

This testing stage is similar in most aspects to Stage 16. Only data associated to $C=0$ were used while the values of σ are free to vary. Other input data are similar to the input data used for Stage 33. A total of 63 hourly recordings were used in computation.

Stage 47

This testing stage is similar in most aspects to Stage 17. Only data associated to $\sigma = 1$ were used in this stage while the values of C are free to vary. Other input data are similar to the input data used for Stage 34. A total of 874 hourly recordings were used in computation.

Stage 48

This testing stage is similar in most aspects to Stage 18. Only data associated to $\sigma = 1$ were used in this stage while the values of C are free to vary. Other input data are similar to the input data used for Stage 34. A total of 95 hourly recordings were used in computation.

Stage 49

This testing stage is similar in most aspects to Stage 18. Other input data are similar to the input data used for Stage 41. A total of 289 hourly recordings were used in computation.

Stage 50

This testing stage is similar in most aspects to Stage 19. Other input data are similar to the input data used for Stage 41. A total of 35 hourly recordings were used in computation.

Stage 51

This testing stage is similar in most aspects to Stage 21. Only data for $C=0$ were used (i.e. the values of the sunshine fraction are free to vary). Other input data are similar to the input data used for

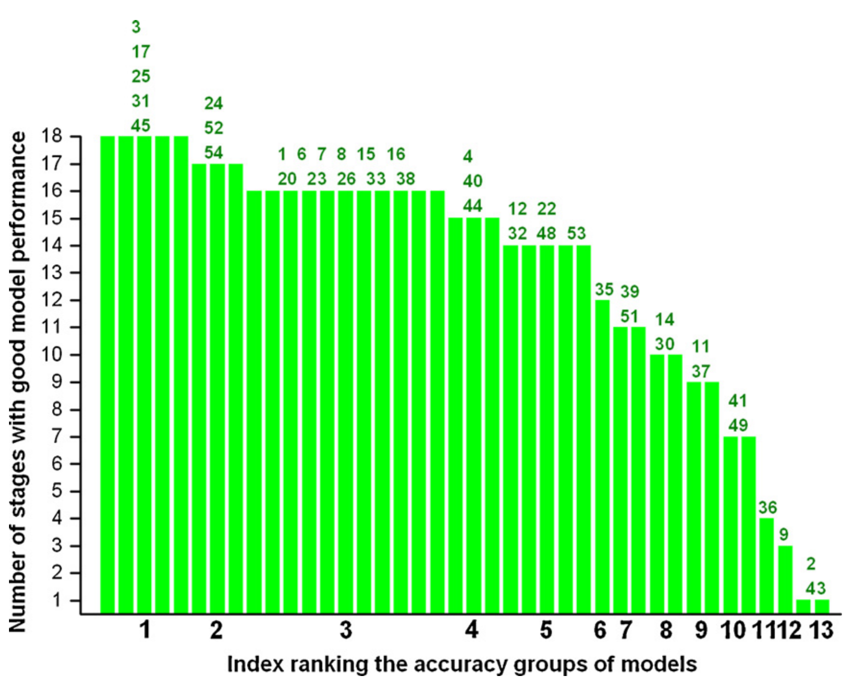


Fig. 3. Same as Fig. 1 for global solar radiation at Bucharest.

Table 10
Models accuracy for computing solar global radiation at Cluj-Napoca and Bucharest.

Color	Meaning
orange	Models obeying both criteria (MBE and RMSE) in both localities
yellow	Models which are simultaneously the best in both localities
purple	Models which are simultaneously the worst in both localities

model	Stages (Cluj-Napoca/Bucarest)																				
	2 32	3 33	4 34	5 35	6 36	7 37	8 38	9 39	10 40	11 41	12 42	13 43	14 44	15 45	16 46	17 47	18 48	19 49	20 50	21 51	22 52
G001	orange	orange		orange	orange	orange	orange	orange	orange	orange	orange	orange		orange				orange		orange	
G002																					
G003	orange	orange		orange	orange	orange	orange	orange	orange	orange	orange	orange		orange				orange		orange	
G004								orange			orange									orange	orange
G005																					
G006	orange	orange		orange	orange	orange	orange	orange	orange	orange	orange	orange		orange				orange		orange	
G007	orange	orange		orange	orange	orange	orange	orange	orange	orange	orange	orange		orange	orange					orange	orange
G008	orange	orange		orange	orange	orange	orange	orange	orange	orange	orange	orange		orange	orange					orange	orange
G009																					
G010																					
G011																					
G012								orange			orange									orange	
G013																					
G014															orange						orange
G015															orange						orange
G016	orange	orange		orange	orange	orange	orange	orange	orange	orange	orange	orange		orange	orange			orange		orange	orange
G017	orange	orange		orange	orange	orange	orange	orange	orange	orange	orange			orange						orange	
G018																					
G019	purple		purple	purple	purple	purple				purple		purple		purple		purple		purple		purple	
G020	orange	orange		orange	orange	orange	orange	orange	orange	orange	orange	orange		orange	orange			orange		orange	orange
G021																					
G022																					
G023		orange			orange		orange	orange	orange		orange			orange	orange					orange	orange
G024		orange			orange		orange	orange	orange	orange	orange			orange	orange			orange	orange	orange	orange
G025		orange			orange		orange	orange	orange	orange	orange		orange	orange	orange			orange	orange	orange	
G026	orange	orange		orange	orange	orange	orange	orange	orange	orange	orange	orange		orange				orange		orange	
G027																					
G028																					
G029																					
G030	orange			orange	orange	orange				orange	orange	orange		orange				orange		orange	
G031	orange	orange		orange	orange	orange	orange	orange	orange	orange	orange	orange	orange	orange				orange	orange	orange	
G032	orange	orange		yellow	orange	orange	orange	orange	orange	orange	orange	orange		orange				orange		orange	
G033	orange	orange			orange		orange	orange	orange	orange	orange	orange		orange	orange			orange		orange	orange
G034																					
G035	orange	orange		orange	orange	orange	orange		orange	orange		orange		orange				orange		orange	
G036																					
G037															orange						
G038		orange			orange		orange	orange	orange	orange	orange			orange	orange			orange		orange	orange
G039																					
G040								orange			orange									orange	orange
G041																					
G042																					
G043																					
G044	orange	orange		orange	orange	orange	orange	orange	orange	orange	orange	orange		orange				orange		orange	
G045	orange	orange		orange	orange	orange	orange	orange	orange	orange	orange	orange		orange				orange		orange	
G046																					
G047													purple		purple				purple		purple
G048		orange						orange	orange		orange									orange	orange
G049	orange			orange	orange	orange				orange		orange						orange			
G050																					
G051													orange		orange				orange		orange
G052	orange	orange		orange	orange	orange	orange	orange	orange	orange	orange	orange	orange	orange				orange	orange		
G053	yellow	orange		orange	orange	yellow	orange	orange	orange	orange	orange	orange		orange				orange		orange	
G054	orange	orange		orange	orange	orange	orange	orange	orange	orange	orange	orange		orange	orange			orange	orange	orange	

Stage 42. A total of 328 hourly recordings were used in computation.

Stage 52

This testing stage is similar in most aspects to Stage 22. Only data for $C = 0$ were used (i.e. the values of the sunshine fraction are free to vary). Other input data are similar to the input data used for Stage 52. A total of 63 hourly recordings were used in computation.

5.2.2. Results

Table 8 shows the models accuracy for computing global radiation at Bucharest. MBE is used as the main accuracy indicator. There is obvious similarity with the results obtained for Cluj-Napoca (compare Tables 8 and 4). First, no model passed the testing stages 4, 17 and 18. Second, very simple models as well as more complex models may belong to the category of “good

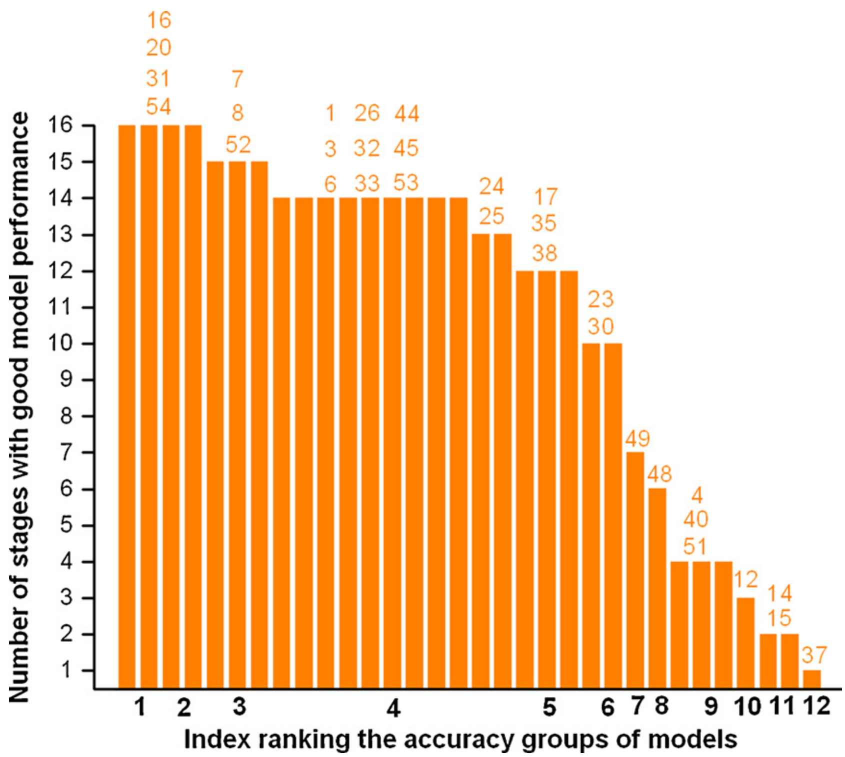


Fig. 4. Same as Fig. 1 for global solar radiation at Cluj-Napoca and Bucharest.

models". Third, models G019 and G047 perform the worst in both cases.

However, visual inspection shows that generally a given model performs better at Bucharest than at Cluj-Napoca (the number of testing stages with accuracy criteria fulfilled is generally larger at Bucharest than at Cluj-Napoca). Also, the category of best models per stage has generally different members in the two locations. Only models G032 and G053 belong to this category in Cluj-Napoca and Bucharest. The other members are G011, G012, G014 and G052 at Cluj-Napoca and G003, G008, G016, G020, G025, G031, G033 and G054 at Bucharest.

Table 9 shows models stratification according to their accuracy for computing global radiation at Bucharest. The best models listed there fulfill the performance criteria for both MBE and RMSE indicators. However, MBE is used there to rank the models.

The very simple model G045 is ranked the second best in stage 44 and the third best in several other stages. Also, the very simple model G036 is ranked the third best at stage 46. This is different from Cluj-Napoca where no single very simple model is ranked among the first three best in the stage testing (see Table 5). Similarly to Cluj-Napoca, the worst performing models are G019 and G047. Among other models ranked between positions 52 and 54 one finds models with complex input dataset but also very simple models (G050 for instance).

Fig. 3 shows the number of testing stages per model with accuracy criteria fulfilled for both MBE and RMSE indicators. This way

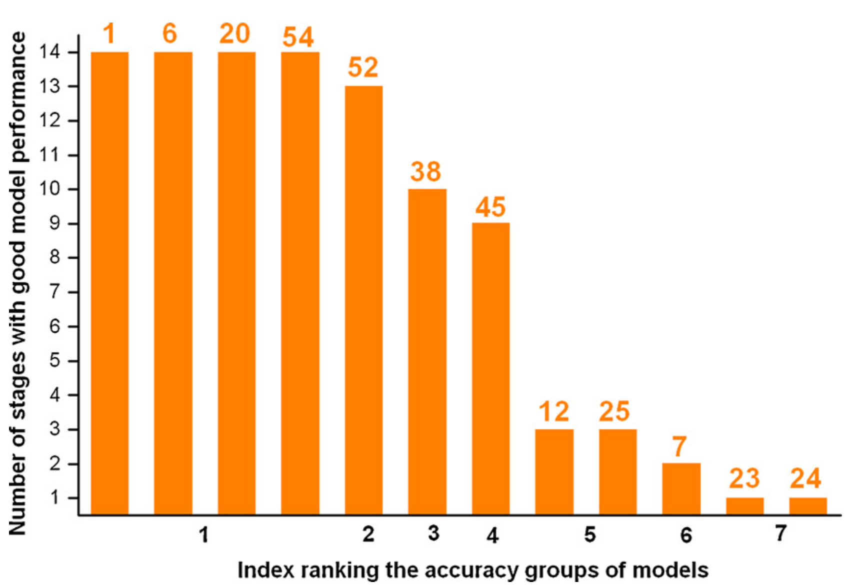


Fig. 5. Same as Fig. 1 for global solar radiation (at Cluj-Napoca and Bucharest) and diffuse solar radiation (at Cluj-Napoca).

Table 11
Models accuracy for computing global radiation (at Cluj-Napoca and Bucharest) and diffuse radiation (at Cluj-Napoca).

Color	Meaning
	Models obeying both criteria (MBE and RMSE) in both localities
■	Models which are simultaneously the worst in both localities

model	Stages (Cluj-Napoca/Bucarest)																				
	2 32	3 33	4 34	5 35	6 36	7 37	8 38	9 39	10 40	11 41	12 42	13 43	14 44	15 45	16 46	17 47	18 48	19 49	20 50	21 51	22 52
G001																					
G002																					
G003																					
G004																					
G005																					
G006																					
G007																					
G008																					
G009																					
G010																					
G011																					
G012																					
G013																					
G014																					
G015																					
G016																					
G017																					
G018																					
G019	■		■	■	■	■				■		■		■		■		■		■	
G020																					
G021																					
G022																					
G023																					
G024																					
G025																					
G026																					
G027																					
G028																					
G029																					
G030																					
G031																					
G032																					
G033																					
G034																					
G035																					
G036																					
G037																					
G038																					
G039																					
G040																					
G041																					
G042																					
G043																					
G044																					
G045																					
G046																					
G047																					
G048																					
G049																					
G050																					
G051																					
G052																					
G053																					
G054																					

of classification stratified the models in several groups and the first thirteen best groups are shown in Fig. 3. Seventeen models belong to the first three best groups. This number is larger than the similar number for Cluj-Napoca (compare Figs. 3 and 1, respectively). Three of the models belonging to the first three best groups (i.e. G001, G006 and G045) are very simple models. This has to be compared with the case of Cluj-Napoca, where only one very simple model (G001) belongs to the first three best groups (see Fig. 1).

5.3. Overall analysis for Cluj-Napoca and Bucharest

An overview of results obtained in both localities is useful. Table 10 shows the models accuracy for computing global radiation at Cluj-Napoca and Bucharest. MBE is used as the main accuracy indicator.

First, no model passed the testing stages 4/34, 17/47 and 18/48. This is a consequence of the results shown in Tables 4 and 8.

Second, four very simple models (i.e. G001, G006, G044 and G045) are good models for some particular stages. Third, models G019 and G047 perform the worst for most stages in both localities. Just two models (G032 and G053) are the best in the two locations, for similar testing stages (i.e. Stages 5/35 for G032 and 2/32 and 7/37 for G053).

Fig. 4 shows the number of testing stages per model with accuracy criteria fulfilled for both MBE and RMSE indicators. This way of classification stratified the models in several groups and the first twelve best groups are shown in Fig. 4. Sixteen models belong to the first three best groups. This number is between the similar numbers for Cluj-Napoca (Fig. 1) and Bucharest (Fig. 3), respectively. However, note that the best three groups in Figs. 1 and 3 refers to 18, 17 and 16 testing stages passed by a given model, respectively, while in Fig. 4 the best three groups refer to 16, 15 and 14 testing stages passed by a given model, respectively. Three models belonging to the first three best groups in Fig. 4 (i.e. G001, G006 and G045) are very simple models.

Table 11 shows the models accuracy for computing global radiation (at Cluj-Napoca and Bucharest) and diffuse radiation (at Cluj-Napoca). MBE is used as the main accuracy indicator. First, no model passed the testing stages 4, 17 and 18. This is a consequence of the results shown in Tables 4 and 8. Second, some very simple models (i.e. G001, G006 and G045) are good models for some particular stages. Third, model G019 perform the worst for most stages in both localities.

There is no single model performing the best in computing both global and diffuse radiation, in both localities, for similar testing stages.

Fig. 5 shows the number of testing stages per model with accuracy criteria fulfilled for both MBE and RMSE indicators. This way of classification stratified the models in several groups and the first seven best groups are shown in Fig. 5. Six models belong to the first three best groups. Note that the best three groups in Fig. 5 refers to 14, 13 and 10 testing stages passed by a given model, respectively. These are considerably low numbers. Compare them with the best three groups when computing global radiation in a single location (i.e. 18, 17 and 16 testing stages passed by a given model; see Figs. 1 and 3). Or, compare them with the best three groups when computing diffuse radiation in a single location (i.e. 18, 16 and 14 testing stages passed by a given model; see Figs. 2). Or, finally, compare them with the best three groups when computing global radiation in two locations (i.e. 16, 15 and 14 testing stages passed by a given model; see Fig. 4).

Three models belonging to the first three best groups in Fig. 5 (i.e. G001, G006 and G045) are very simple models.

6. Conclusions

Fifty-four broad band models for computation of global and diffuse irradiance on horizontal surface were selected. These models were tested by using input data from two meteorological stations from Romania (South-Eastern Europe), i.e. Cluj-Napoca and Bucharest. The input data consist of surface meteorological data, column integrated data and data derived from satellite measurements. The testing procedure is performed in forty-two stages intended to provide information about the sensitivity of the models to various sets of input data.

Looking to the results for global radiation computation at Cluj-Napoca, one sees that nine models belong to the first three best groups. One of these models (i.e. G001) is a very simple model. However, no single very simple model is ranked among the first three best models in the stage testing. In case of computing diffuse radiation, the number of “good” models is smaller than when computing global radiation. Also, no very simple model is ranked the first best model in a particular testing stage. However, three models of the first nine best groups (i.e. G001, G002 and G006) are very simple models. Model G029 gives the best results to compute diffuse radiation for most testing stages. The best models for solar diffuse radiation computation are, on equal-footing, G002 and G027. The second best model is G029.

Looking to the results for global radiation computation at Bucharest, the models perform generally better than at Cluj-Napoca. Indeed, in Bucharest seventeen models belong to the first three best groups. But the category of best models per stage has generally different members in the two locations. Three of the models belonging to the first three best groups in Bucharest (i.e. G001, G006 and G045) are very simple models.

Looking to the combined results for global radiation computation at Cluj-Napoca and Bucharest, one sees that sixteen models belong to the first three best groups. Three models belonging to the first three best groups (i.e. G001, G006 and G045) are very simple models. Only two models (G032 and G053) are the best in both locations, for one or two testing stages. The best models for solar global radiation computation are, on equal-footing, G016, G020, G031 and G054. The second best models are, on equal-footing, G007, G008 and G052.

Looking to the combined results for global and diffuse radiation computation at Cluj-Napoca and Bucharest, the following conclusions can be drawn. There is no single model performing the best in computing both global and diffuse radiation, in both localities, for similar testing stages. Six models belong to the first three best groups. Three models belonging to the first three best groups in Fig. 5 (i.e. G001, G006 and G045) are very simple models. The best models for computation of both global and diffuse radiation are, on equal-footing, G001, G006, G020 and G054. The second best model is G052.

We may conclude that models’ accuracy depends on the set of input data. There is no model to be ranked “the best” for all sets of input data. Very simple models as well as more complex models may belong to the category of “good models” but generally the last models perform better.

Detailed information about the performance of each model is provided in [11,12].

Acknowledgments

This work was supported in part by a grant of the Romanian National Authority for Scientific Research, CNCS – UEFISCDI, project number PN-II-ID-PCE-2011-3-0089 and by the European Cooperation in Science and Technology project COST ES1002.

References

[1] Davies JA, McKay DC, Luciani G, Abdel-Wahab M. Validation of models for estimating solar radiation on horizontal surfaces. Downsview, Ontario: Atmospheric Environment Service; 1988. IEA Task IX Final Report.
[2] Davies JA, McKay DC. Evaluation of selected models for estimating solar radiation on horizontal surfaces. Solar Energy 1989;43:153–68.
[3] Gueymard C. Critical analysis and performance assessment of clear sky solar irradiance models using theoretical and measured data. Solar Energy 1993;51:121–38.
[4] Badescu V. Verification of some very simple clear and cloudy sky models to evaluate global solar irradiance. Solar Energy 1997;61:251–64.
[5] Batlles FJ, Olmo FJ, Tovar J, Alados-Arboledas L. Comparison of cloudless sky parameterizations of solar irradiance at various Spanish midlatitude locations. Theor Appl Climatol 2000;66:81–93.
[6] Iziomon MG, Mayer H. Assessment of some global solar radiation parameterizations. J Atmos Solar Terr Phys 2002;64:1631–43.
[7] Ineichen P. Comparison of eight clear sky broadband models against 16 independent data banks. Solar Energy 2006;80:468–78.
[8] Younes S, Muneer T. Clear-sky classification procedures and models using a world-wide data-base. Appl Energy 2007;84:623–45.
[9] Gueymard CA, Myers DR. Validation and ranking methodologies for solar radiation models. In: Badescu V, editor. Modeling solar radiation at the earth surface. Berlin: Springer; 2008. p. 479–509 [chapter 20].

[10] Gueymard CA, Clear-sky solar irradiance predictions for large-scale applications using 18 radiative models: improved validation methodology and detailed performance analysis, Solar Energy, in press.
[11] Badescu V, Gueymard CA, Cheval S, Oprea C, Baciu M, Dumitrescu A, et al. Accuracy and sensitivity analysis for 54 clear-sky solar radiation models using routine hourly global irradiance measurements in Romania, submitted for publication.
[12] Badescu V, Gueymard CA, Cheval S, Oprea C, Baciu M, Dumitrescu A, et al. Accuracy and sensitivity analysis for fifty-four models of computing solar diffuse hourly irradiation on clear sky, submitted for publication.
[13] Badescu V, Cheval S, Gueymard C, Oprea C, Baciu M, Dumitrescu A, et al. Testing 52 models of clear sky solar irradiance computation under the climate of Romania. In: The workshop solar energy at urban scale. 2010. p. 12–5.
[14] Gueymard CA, Kambezidis HD. Solar spectral radiation. In: Muneer T, editor. Solar radiation and daylight models. New York: Elsevier; 2004.
[15] ASHRAE. Handbook of fundamentals. Atlanta, GA: American Society of Heating, Refrigerating and Air-Conditioning Engineers Inc.; 1972.
[16] ASHRAE. Handbook fundamentals. Atlanta, GA: American Society of Heating, Refrigerating and Air-Conditioning Engineers Inc.; 2005 [chapter 31].
[17] Badescu V. Use of sunshine number for solar irradiance time series generation. In: Badescu V, editor. Modeling solar radiation at the Earth surface. Berlin: Springer; 2008. p. 327–55 [chapter 13].
[18] Bashahu M, Laplaze D. An atmospheric model for computing solar radiation. Renew Energy 1994;4:455–8.
[19] King R, Buckius RO. Direct solar transmittance for a clear sky. Solar Energy 1979;22:297–301.
[20] Barbaro S, Coppolino S, Leone C, Sinagra E. An atmospheric model for computing direct and diffuse solar radiation. Solar Energy 1979;22:225–8.
[21] Badescu V. Can the model proposed by Barbaro et al. be used to compute global solar radiation on the Romanian territory? Solar Energy 1987;38: 247–54.
[22] Biga AJ, Rosa R. Contribution to the study of the solar radiation climate of Lisbon. Solar Energy 1979;23:61–7.
[23] Bird RE, Hulstrom RL, Direct insolation models, Solar Energy Research Institute (now NREL), Golden CO, SERI/TR-335-344; 1980.
[24] Bird RE, Hulstrom RL. Review, evaluation, and improvement of direct irradiance models. Trans ASME, J Sol Engng 1981;103:182–92.
[25] Gueymard C. Direct solar transmittance and irradiance predictions with broadband models. Part I: detailed theoretical performance assessment. Solar Energy 2003;74:355–79.
[26] Atwater MA, Ball JT. A numerical solar radiation model based on standard meteorological observations. Solar Energy 1978;21:163–70.
[27] Atwater MA, Ball JT. Erratum. Solar Energy 1979;23:275.
[28] Chandra M. Dependence of solar radiation availability on atmospheric turbidity. Proc ISES Conf 1978:430–4.
[29] Hinzpeter H. Uber Trubungsbestimmungen in Potsdam in dem Jahren 1946 und 1947 m. Meteor 1950;4:1.
[30] Katz M, Baille A, Mermier M. Atmospheric turbidity in a semi-rural site. Part I: evaluation and comparison of different atmospheric turbidity coefficients. Solar Energy 1982;28:323–7.
[31] Abdelrahman MA, Said SAM, Shuaib AN. Comparison between atmospheric turbidity coefficients of desert and temperate climates. Solar Energy 1988;40:219–25.
[32] Grenier JC, de la Casiniere A, Cabot T. A spectral model of Linke's turbidity factor and its experimental implications. Solar Energy 1994;52:303–14.
[33] Iqbal M. An Introduction to solar radiation. Toronto: Academic Press; 1983.
[34] Suckling PW, Hay JE. Modeling direct, diffuse and total solar radiation for cloudless days. Atmosphere 1976;14:298–308.
[35] Suckling PW, Hay JE. A cloud layer-sunshine model for estimating direct, diffuse and total solar radiation. Atmosphere 1977;15:194–207.
[36] Gueymard C. A two-band model for the calculation of clear sky solar irradiance, illuminance, and photosynthetically active radiation at the earth's surface. Solar Energy 1989;43:253–65.
[37] Dogniaux B, Programme de calcul des eclairements solaires energetiques et lumineux de surfaces orientees et inclinees, Rep. 14, IRM, Brusels; 1976.
[38] Dogniaux B, Variations qualitatives et quantitatives des composantes du rayonnement solaire sur une surface horizontale par ciel serein en fonction du trouble atmospherique, Rep. B62, IRM, Brusels; 1970.
[39] Dogniaux B, Variations geographiques et climatiques des expositions energetiques solaires sur des surfaces receptrices horizontales et verticales, Rep. B38, IRM, Brusels; 1975.
[40] Goswami TK, Klett DE, Comparison of several models for long term monthly average daily insolation on horizontal surfaces and the estimation of horizontal surface insolation for 16 U.S. locations, ASME paper 80-WA/Sol-28; 1980.
[41] Festa R, Ratto CF, Solar radiation statistical properties, Rep. IEA-SCHP-9E-4, IEA Task IX, International Energy Agency; 1993.
[42] Daneshyar M. Solar radiation statistics for Iran. Solar Energy 1978;21:345–9.
[43] Paltridge GW, Proctor D. Monthly mean solar radiation statistics for Australia. Solar Energy 1976;18:235–43.
[44] Kreith F, Kreider JF. Solar heating and cooling. Washington: Scripta Book Co.; 1975.
[45] Rigollier C, Bauer O, Wald L. On the clear sky model of the ESRA—European Solar Radiation Atlas—with respect to the Heliosat method. Solar Energy 2000;68:33–48.
[46] ESRA, Helioclim, Lectures 2010 (http://www.helioclim.net/publications/index.html#esra).
[47] Remund J, Wald L, Lefevre M, Ranchin T, Page J. Worldwide Linke turbidity information. In: Proceedings of the ISES conference. 2003.
[48] Remund J, pers. commm.; 2006.
[49] Molineaux B, Ineichen P, O'Neill N. Equivalence of pyrheliometric and monochromatic aerosol optical depths at a single key wavelength. Appl Opt 1998;37:7008–18.
[50] Dogniaux R. The estimation of atmospheric turbidity. In: Proc Advan European Solar Radiation Climatol London UK, UK Int Sol Energy Soc. 1986. p. 3.1–4.
[51] Hottel HC. A simple model for estimating the transmittance of direct solar radiation through clear atmospheres. Solar Energy 1976;18:129–34.
[52] De Carli F, Groppi C, Festa R, Ratto CF. A procedure to obtain global radiation maps from sunshine durations at isolated stations in a region with complex orography. Solar Energy 1986;37:91–108.
[53] Jafarpur K, Yaghoubi MA. Solar radiation for Shiraz, Iran. Solar Wind Technol 1989;6:177–9.
[54] Aziz GMA. Estimation of hourly clear-sky solar radiation for P.D.R. Yemen. Solar Wind Technol 1990;7:255–60.
[55] Khalil A, Alnajjar A. Experimental and theoretical investigation of global and dffuse solar radiation in the United Arab Emirates. Renew Energy 1995;6:537–43.
[56] Toğrul IT, Toğrul H, Evin D. Estimation of global solar radiation under clear sky radiation in Turkey. Renew Energy 2000;21:271–87.
[57] Liu BYH, Jordan RC. The interrelationship and characteristic distribution of direct, diffuse and total solar radiation. Solar Energy 1960;4:1–12.
[58] Ideriah FJK. A model for calculating direct and diffuse solar radiation. Solar Energy 1981;26:447–52.
[59] Ineichen P. A broadband simplified version of the Solis clear sky model. Solar Energy 2008;82:758–62.
[60] Davies JA. Estimating global solar radiation. Bound Layer Meteor 1975;9:33–52.
[61] Hoyt DV. A model for the calculation of global solar radiation. Solar Energy 1978;21:27–35.
[62] Josefsson W, Modeling direct and global radiation from hourly synoptic observations, unpublished manuscript; 1985.
[63] Kasten F. Parametrisierung der Globalstrahlung durch Bedeckungsgrad und Trübungsfaktor. Ann Met 1983;20:49–50.
[64] Krarti M, Huang J, Seo D, Dark J. Development of solar radiation models for tropical locations, final report for Research Project 1309-RP. Atlanta, GA: American Society of Heating, Refrigerating and Air-Conditioning Engineers Inc.; 2006.
[65] Buckius RO, King R. Diffuse solar radiation on a horizontal surface for a clear sky. Solar Energy 1978;21:503–9.
[66] Zhang Q, Huang J, Lang S. Development of typical year weather data for Chinese locations. ASHRAE Trans 2002:108.
[67] Watanabe T, Urano Y, Hayashi H. Procedures for separating direct and diffuse insolation on a horizontal surface and prediction of insolation on tilted surface. Trans Architectural Inst Jpn 1983;330:96–108.
[68] Davies JA, Uboegbulam TC. Parameterization of surface incoming radiation in tropical cloudy conditions. Atmos-Ocean 1979;17:14–23.
[69] Machler MA, Iqbal M. A modification of the ASHRAE clear sky irradiation model. ASHRAE Trans Part IA 1985;106–115.
[70] Maxwell EL. METSTAT—The solar radiation model used in the production of the National Solar Radiation Data Base (NSRDB). Solar Energy 1998;62:263–79.
[71] Muneer T, Gul M, Kambezedis H. Evaluation of an all-sky meteorological radiation model against long-term measured hourly data. Energy Convers Mgmt 1998;39:303–17.
[72] Kambezidis H, pers. comm.; 2002.
[73] Muneer T. Solar radiation and daylight models. New York: Elsevier; 2004.
[74] Gueymard CA. Direct solar transmittance and irradiance predictions with broadband models. Part 2: validation with high-quality measurements. Solar Energy 2003;74:381–95. Corrigendum: Solar Energy 76 (2004) 515.
[75] Kambezidis H, Psiloglou BE, pers. comm.; 2007.
[76] Kambezidis H, Psiloglou BE. The Meteorological Radiation Model (MRM): advancements and applications. In: Badescu V, editor. Modeling solar radiation at the Earth's surface. Recent advances. Berlin: Springer; 2008. p. 357–92 [chapter 14].
[77] Nijegorodov N, Adedoyin JA, Devan KRS. A new analytical-empirical model for the instantaneous diffuse radiation and experimental investigation of its validity. Renew Energy 1997;11:341–50.
[78] Nijegorodov N, Luhanga PVC. Air mass: analytical and empirical treatment; an improved formula for air mass. Renew Energy 1996;7:57–65.
[79] Belcher BN, DeGaetano AT. Integration of ASOS weather data into model-derived solar radiation (1226-RP). ASHRAE Trans 2005;111(1):363–78.
[80] Belcher BN, DeGaetano AT. A revised empirical model to estimate solar radiation using automated surface weather observations. Solar Energy 2007;81:329–45.
[81] Belcher B, pers. commun.; 2005.
[82] Paltridge GM, Platt CMR. Radiative processes in meteorology and climatology. New York: Elsevier; 1976.
[83] Ch. Perrin de Brichambaut, Ch Vauge, Le gisement solaire, Evaluation de la ressource énergétique, Lavoisier, Technique et Documentation, Paris; 1982.

[84] Psiloglou BE, Santamouris M, Asimakopoulos DN. Atmospheric broadband model for computation of solar radiation at the Earth's surface. Application to mediterranean climate. P Appl Geophys 2000;157:829–60.
[85] B.E. Psiloglou (pers. comm. 2006).
[86] Gueymard CA. REST2: high performance solar radiation model for cloudless-sky irradiance, illuminance and photosynthetically active radiation—validation with a benchmark dataset. Solar Energy 2008;82:272–85.
[87] Rodgers GG, Souster CG, Page KJ. The development of an interactive computer program SUN1 for the calculation of solar irradiances and daily irradiations on horizontal surfaces on cloudless days for given conditions of sky clarity and atmospheric water content, Rep. BS28, Univ. of Sheffield; 1978.
[88] Carroll JJ. Global transmissivity and diffuse fraction of solar radiation for clear and cloudy skies as measured and as predicted by bulk transmissivity models. Solar Energy 1985;35:105–18.
[89] Robinson N, editor. Solar radiation. Amsterdam: Elsevier; 1966.
[90] Sellers WD. Physical climatology. Univ Chicago Press 1965.
[91] Santamouris M, pers comm.; 2006.
[92] Schulze RE. A physically based method of estimating solar radiation from suncards. Agric Meteorol 1976;16:85–101.
[93] Sharma MR, Pal RS. Interrelationships between total, direct, and diffuse solar radiation in the tropics. Solar Energy 1965;9:183–92.
[94] Watt D, On the nature and distribution of solar radiation, Report for U.S. DOE; 1978.
[95] Wesely ML, Lipschutz RC. An experimental study of the effects of aerosols on diffuse and direct solar radiation received during the summer near Chicago. Atmos Environ 1976;10:981–7.
[96] Wesely ML, Lipschutz RC. A method for estimating hourly averages of diffuse and direct solar radiation under a layer of scattered clouds. Solar Energy 1976;18:467–73.
[97] Yang K, Huang GW, Tamai N. A hybrid model for estimating global solar radiation. Solar Energy 2001;70:13–22.
[98] Yang K, Koike T, Ye B. Improving estimation of hourly daily and monthly solar radiation by importing global data sets. Agric Forest Meteorol 2006;137:43–55.
[99] Zhang Q. Development of the typical meteorological database for Chinese locations. Energy Build 2006;38:1320–6.
[100] Zhang Q, pers. comm.; 2008.
[101] Hourwitz B. Insolation in relation to cloudiness and cloud density. J Met 1945;2:154–6.
[102] Hourwitz B. Insolation in relation to cloud type. J Met 1946;3:123–4.
[103] Adnot J, Bourges B, Campana D, Gicquel R. Utilisation desc courbes de frequence cumulees pour le calcul des installation solaire. In: Lestienne R, editor. Analyse statistique des processus meteorologiques appliquee a l'energie solaire. Paris: CNRS; 1979. p. 9–40.
[104] Paulescu M, Schlett Z. A simplified but accurate spectral solar irradiance model. Theor Appl Climatol 2003;75:203–12.
[105] Paulescu M, pers. comm.; 2009.
[106] Janjai S, Models for estimating direct normal and diffuse irradiances clear sky condition, Technical report, Nakhonpathom, Thailand: Department of Physics, Silpakorn University; 2010.
[107] Janjai S, Sricharoen K, Pattarapanitchai S, Semi-empirical models for the estimation of clear sky solar global and direct normal irradiances in the tropics. Appl Energy (July 2011) doi:10.1016/j.apenergy.2011.06.021.
[108] Myers DR, Wilcox SM. Relative accuracy of 1-minute and daily total solar radiation data for 12 global and 4 direct beam solar radiometers. In: American solar energy society annual conference. 2009.
[109] WMO, Guide to meteorological instruments and methods of observation, WMO No. 8, 2008, Ch. 8–Measurement of sunshine duration, pp. I.8.1-1.8.11; <http://www.wmo.int/pages/prog/www/IMOP/publications/CIMO-Guide/CIMO_Guide-7th_Edition-2008.html>.
[110] Schulz J, Albert P, Behr H-D, Caprion D, Deneke H, Dewitte S, et al. Operational climate monitoring from space: the EUMETSAT Satellite Application Facility on Climate Monitoring (CM-SAF). Atmos Chem Phys 2009;9:1687–709, http://www.atmos-chem-phys.org/9/1687/2009/acp-9-1687-2009.pdf.
[111] Gueymard CA, Thevenard D. Monthly average clear-sky broadband irradiance database for worldwide solar heat gain and building cooling load calculations. Solar Energy 2009;83(11):1998–2018.
[112] Leckner B. The spectral distribution of solar radiation at the Earth's surface – elements of a model. Solar Energy 1978;20:143–50.